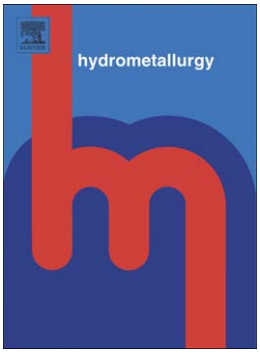

Electrochemical oxidation of iron(II) ions on lead alloy anodes

V. Tjandrawan, M.J. Nicol

PII: S0304-386X(12)00226-5
DOI: doi: 10.1016/j.hydromet.2012.10.009
Reference: HYDROM 3623

To appear in: *Hydrometallurgy*

Received date: 11 September 2012
Revised date: 22 October 2012
Accepted date: 23 October 2012

Please cite this article as: Tjandrawan, V., Nicol, M.J., Electrochemical oxidation of iron(II) ions on lead alloy anodes, *Hydrometallurgy* (2012), doi: 10.1016/j.hydromet.2012.10.009

Electrochemical oxidation of iron(II) ions on lead alloy anodes

V. Tjandrawan and M. J. Nicol*

School of Chemical and Mathematical Sciences, Murdoch University, Murdoch, WA 6150, Australia

Abstract

The anodic oxidation of iron(II) ions on Pb-Ca-Sn anodes in sulphate solutions have been studied using cyclic voltammetry and potentiostatic methods. The oxidation of iron(II) on these anodes does not occur on a lead sulphate surface but occurs readily on a lead dioxide surface. The rate of the oxidation of iron(II) at the anodes is controlled by mass transport to the anode surface. Chemical reaction between iron(II) and PbO_2 on the surface of the anodes is rapid. In the presence of manganese ions, oxidation of iron(II) also occurs on the surface of manganese oxides which can also rapidly oxidise iron(II). The presence of iron(II) in the electrolyte will increase the rate of "sulfation" of anodes during power disruptions in copper tankhouses. Limited experiments with a Pb-Ag anode showed very similar results.

Keywords: electrowinning; copper; anode; lead; oxidation; iron(II)

* *Corresponding author. Tel: +61 8 9360 6766; E-mail address: m.nicol@murdoch.edu.au*

1. Introduction

Iron(II) is present as a major impurity (1 to 5 g L^{-1}) in electrolytes used in the electrowinning of copper and as a minor impurity (less than 1 mg L^{-1}) in the electrowinning of zinc and nickel. It was considered useful to study the anodic oxidation of iron(II) ions in order to compare with that of the oxidation of manganese(II) ions which are present in zinc electrolytes (2 to 10 g L^{-1}) and also copper and nickel electrolytes (less than 200 mg L^{-1}). The anodic characteristics of the oxidation of manganese are difficult to study as the reactions are masked by the oxidation of the alloy surface and the evolution of oxygen. Finally, it is of interest to establish the extent to which anodic reactions are possible on these anode materials in the potential region between formation of lead sulphate and its oxidation to one of several possible lead dioxide phases. As will be demonstrated, the oxidation of iron(II) provides a convenient method for probing the reactions involved in the oxidation of lead alloy anodes.

Although oxidation of iron(II) on the anodes during the electrowinning of copper is well known as contributing to a loss of current efficiency due to simultaneous reduction of iron(III) on the cathodes, little has been published on the kinetics of the reaction on lead alloy anodes. It has been reported that the oxidation of iron(II) on Pb-Sb alloy mesh electrodes is retarded compared to PbO_2-coated Ti anodes and that it occurred simultaneously with the evolution of oxygen (Dew and Phillips, 1985). The oxidation of iron(II) was used as a method for characterizing mass transfer to a concentric cylinder reactor in a publication by El-Sherbiny et al. (1991) which described the use of a PbO_2 – coated anode. However, no details of anodic reaction were investigated. In another study (Kolodziej and Adamski, 1985), manganese ions were added to the electrolyte to increase the corrosion resistance of pure lead anodes used for the oxidation of iron(II). Again, no details

of the kinetics of the anodic reaction were presented. Oxidation of iron(II) on several anode materials was evaluated by Cifuentes and Glasner (2003) and the current- potential curves for a pure lead anode showed no oxidation of iron(II) at potentials below that at which oxygen evolution occurred.

As part of a wider study of the reactions occurring on lead alloy anodes during the electrowinning of base metals, this paper will focus on the anodic oxidation of iron(II) in sulphate solutions at anodes typically used in the electrowinning of copper and zinc.

2. Material and methods

The electrochemical studies were performed using a conventional three-electrode system. A modified thermostatted Metrohm glass cell covered with a detachable lid was used as a reaction vessel. The working electrode was a rotating disc (5 mm diameter) of either Pb-0.08%Ca-1.3%Sn-0.01%Al rolled alloy or rolled Pb-0.42%Ag alloy. Rotating disk electrodes were core-drilled from 9 mm commercial alloy sheets and the cylinders were attached to stainless steel stubs with conducting silver epoxy and subsequently coated with an insulating epoxy resin. The reference electrode was a $Hg|Hg_2SO_4$ (saturated K_2SO_4) electrode (MSE, E = +0.645 V versus standard hydrogen electrode, SHE) which was joined to the main cell by a Luggin capillary passing through a screw fitting in the base of the cell. The tip of the Luggin capillary was placed ~0.5 cm below the surface of the working electrode. The counter electrode was a platinum wire. All potentials are reported with respect to SHE.

The rotating disc electrode (RDE) was rotated using a drive consisting of an optically controlled unit coupled to a dc motor. Unless stated otherwise, the electrodes were rotated at 500 rev min^{-1}. Electrochemical experiments were

carried out using a Solartron potentiostat operated with corrosion measurement software. The temperature of the electrolyte was maintained at 40±0.1ºC. Prior to all tests, the exposed surface of the working electrode was wet-polished using 800 followed by 1200 silicon carbide papers and rinsed with deionised water.

Sulphuric acid (150 g L^{-1}), iron(II) solutions of various concentrations (5 and 10 g L^{-1}) and manganese(II) solutions of various concentrations (0.1 and 1 g L^{-1}) were prepared using AR grade 98% sulphuric acid, ferrous sulphate heptahydrate, manganese sulphate and Milli-Q distilled water.

3. Results and discussion

3.1 Anodic reactions in the absence of iron(II)

In order to compare the anodic reactions in the presence of iron(II) ions, a limited study was made of the anodic behaviour in the absence of iron(II) and Fig. 1 shows the cyclic voltammograms of each of the rotating alloy electrodes in a solution of 150 g L^{-1} sulphuric acid at 40 ^{o}C. The sweeps were initiated in a positive direction from the rest potentials which were close to -0.4 V at a scan rate of 1 mV s^{-1}.

Oxidation of lead to a passivating surface of $PbSO_4$ occurs in peak (a).

$PbSO_4 + H^+ + 2e^- = Pb + HSO_4^-$ $\quad E^o = -0.304$ V at 40^{o}C (1)

Further oxidation during the positive sweep is observed in peak (b) at about 1.8 V which has been attributed to the oxidation of $PbSO_4$ to α- and β-PbO_2.

$PbO_2 + HSO_4^- + 3H^+ + 2e^- = PbSO_4 + 2H_2O$ $\quad E^o = 1.626$ V at 40^{o}C (2)

This is followed at higher potentials by the evolution of oxygen. Although reaction (2) is written as a direct oxidation of $PbSO_4$, the actual mechanism has been described by Pavlov and Dinev (1980) as involving dissolution of $PbSO_4$

crystals and oxidation of Pb^{2+} ions at the lead surface to PbO_2 which grows as a fine needle-like deposit in the intercrystalline spaces between the $PbSO_4$ crystals.

As the potential sweep is reversed, two cathodic peaks are observed which are due to the reduction of PbO_2 to $PbSO_4$ at 1.6 to 1.5 V (peak (d)) followed by that of PbO and $PbSO_4$ to Pb at -0.1 to -0.6 V (peaks (e)) with an inactive region between 1.4 to -0.1 V (Sharpe, 1977). The appearance of an unusual anodic current peak (c) at about 1.6 V has been attributed by Sharpe (1977) to the oxidation of lead metal exposed in the process of reduction of PbO_2 to $PbSO_4$. The net charge involved in the reactions in this region from 1.65 to 1.4 V is positive for both electrodes.

A typical current-time transient obtained on a Pb-Ca-Sn anode at a potential of 1.8 V is shown in Fig. 2. At this potential, the partial current density due to the evolution of oxygen is negligible (less than 0.5 A m^{-2}) and the observed currents are due to the oxidation of the alloy (Tjandrawan and Nicol, 2010).

The peak after about 200 seconds has been attributed by Ruetschi and Angstadt (1964) to the nucleation and growth of a PbO_2 phase in the outer, acidic part of the corrosion layer. After 1 hour, the potential was switched to 1.4 V i.e. below that for reduction of PbO_2 to $PbSO_4$. The resulting net current is anodic and significantly greater than that at 1.8 V after 1 hour. One interpretation of this unusual phenomenon is that so-called "self-discharge" of the PbO_2 at the metal/PbO_2 interface by the reaction

$$PbO_2 + Pb + 2HSO_4^- + 2H^+ = 2PbSO_4 + 2H_2O \quad (3)$$

which occurs by a dissolution/precipitation reaction, exposes the alloy surface which can undergo oxidation to $PbSO_4$. Details of these processes are beyond the scope of this report.

It is generally believed that the composition of the layers on anodized lead surfaces varies with the potential as shown in Fig. 3. The equilibrium potentials of the various couples involved are also shown.

In terms of this model, the anodic film at potentials below about 1.65 V (1.0 V versus MSE), consists of a protective lead sulphate layer or membrane with tetragonal PbO and/or α-PbO_2 between the alloy surface and the membrane which is permeable to protons but not sulphate or lead ions. This results in the electrolyte inside the membrane becoming depleted in protons with the formation of PbO and PbO_2. At potentials above about 1.7 V, oxidation to β-PbO_2 occurs as described above.

3.2 Anodic reactions in the presence of iron(II)

Cyclic voltammograms (Fig. 4) were obtained with both rotating alloy disk anodes at 1 mV s^{-1} in a solution containing 150 g L^{-1} H_2SO_4 and 10 g L^{-1} Fe(II) at 40 °C. The scan was started in a positive direction from the open circuit potential at about -0.35 V and reversed at a potential of about 2.1 V.

Oxidation of iron(II) could be expected at potentials above about 0.7 V given that the formal reduction potential for the reaction

$$Fe^{3+} + e^- = Fe^{2+} \qquad (4)$$

is 0.69 V under these conditions. However, no significant anodic currents are obtained until the potential increased to about 1.5 V in the case of the Pb-Ca-Sn anode. This confirms that oxidation of the passive $PbSO_4$ layer to electroactive α- and/or β-PbO_2 is a prerequisite for oxidation of iron(II). Simultaneous evolution of oxygen occurs at higher potentials. In the case of the Pb-Ag anode, oxidation to PbO_2 coincided with simultaneous evolution of oxygen at potentials above 2.0 V.

On the reverse scan, the current decreases rapidly to a steady limiting value of about 620 A m^{-2} on both alloy electrodes at potentials between 1.5 and 2.0 V. The limiting current density for the oxidation of iron(II) under these conditions can be estimated from the Levich equation to be 620 A m^{-2} (diffusion coefficient of iron(II) of 4.9 x 10^{-6} cm^2 s^{-1} (Li and Miller, 2007) at 25 ^oC was corrected to 40 ^oC using an activation energy of 20 kJ mol^{-1}). These observations suggest that oxidation of iron(II) only occurs on the surface of the lead dioxide phases. The steep decrease of the current from the plateau at about 1.5 V coincides with the potential at which PbO_2 is reduced to $PbSO_4$ as shown in Fig. 1. The small peaks at potentials between 1.5 and 1.6 V coincide with those in Fig. 1 and will be discussed in more detail below.

Confirmation of mass transport-controlled oxidation of iron(II) is given by the results in Fig. 5 which show that the limiting current plateau at potentials between 1.5 and 2.0 V is consistent with values calculated from the Levich equation at different rotation speeds and concentrations of iron(II).

The effect of increasing the anodic limit of the sweep on the oxidation of iron(II) is summarized by the results in Fig. 6 which shows in more detail the curves at high potentials. The positive hysteresis at all potential limits of 1.625 V and above suggests that the oxidation of $PbSO_4$ occurs at potentials as low as 1.625 V but at a relatively low rate. This conclusion was arrived at from a voltammetric study of the anodic behaviour of lead in sulfuric acid solutions in the absence of iron(II) (Pavlov and Dinev, 1980). The curve for 1.75 V reveals two peaks in the reverse sweep suggesting that oxidation of iron(II) on the β-PbO_2 formed at the higher potential of about 1.7 V is more rapid than that on α-PbO_2 formed at the lower potential of about 1.6 V as suggested in Fig. 3.

The slow formation of the PbO_2 surface layer is such that the limiting current density for oxidation of iron(II) is only reached at the positive potential limit of 1.9 V. The apparent increase in the limiting current at potentials above about 1.95 V is possibly due to increased turbulence created by the presence of oxygen bubbles on the surface formed at potentials where oxygen evolution is visible. The peak at a potential of about 1.56 V followed by a small negative peak at 1.53 V correspond those observed in the absence of iron(II) as seen in Fig. 1. The rapid reduction of the rate of oxidation of iron(II) at these potentials during the reverse sweep contrasts with the slow increase in the rate during the forward sweep i.e. reduction of PbO_2 to $PbSO_4$ is considerably more reversible than the reverse reaction. The decrease in the current on the reverse sweep at potentials more positive than those required for the reduction of PbO_2 for the experiments with positive potential limits below 1.9 V suggests that the rate of the reaction

$$PbO_2 + 2Fe^{2+} + HSO_4^- + 3H^+ = PbSO_4 + 2Fe^{3+} + 2H_2O \quad (5)$$

on the PbO_2 surface is such that regeneration of PbO_2 is not rapid enough at potentials below about 1.8 V.

The slow conversion of $PbSO_4$ to PbO_2 is further shown by the current-time transients in Fig. 7 for potentiostatic experiments at various potentials. The current decays rapidly at short times before increasing slowly to the limiting current at long times. The limiting current for oxidation of iron(II) is achieved at all potentials. The higher limiting currents shown for potentials of 1.95 and 2.0 V are due to the simultaneous evolution of oxygen.

The transients during the first minute are shown in Fig. 8. It is apparent that the current decays at the roughly the same rate at all potentials to a constant value of about 10 A m^{-2} irrespective of the presence of iron(II) ions. It is suggested that

this decay corresponds to the oxidation of lead to the passive $PbSO_4$ layer with the current in the absence of iron(II) decaying to almost zero at longer times.

Analysis of the rising portions of the transients in Fig. 7 showed that a plot of an empirical equation $\ln(1/i - 1/i_L)$ in which i_L is the limiting current density was linear at all potentials and the slopes of these lines are plotted in Fig. 9. These transients describe the rate of the nucleation and growth of the PbO_2 phases on the $PbSO_4$ surface. It is interesting to note that there appears to be different trends below and above about 1.7 V which could be ascribed to the formation of the α–PbO_2 phase at the lower potentials and β–PbO_2 at potentials above about 1.7 V. This is consistent with the two peaks observed in Fig. 6 when the sweep direction was reversed at 1.75 V.

It is not possible to estimate the charge involved in the oxidation of the alloy in the presence of iron(II) but in the case of the experiment conducted at 1.7 V in the absence of iron(II), the accumulated charge during oxidation for 1 hour was found to be 5460 C m^{-2} which, for a 4-electron process is equivalent to 0.0141 mol PbO_2 m^{-2} assuming that the rate of oxygen evolution is negligible at this potential. If the rate of reaction (4) is controlled by mass transport of iron(II) ions to the surface of the PbO_2 layer, it can be calculated from the limiting current density of 400 A m^{-2} for an iron(II) concentration of 5 g L^{-1} at 800 rpm that the PbO_2 layer would be reduced by reaction (5) in some 13.5 seconds.

Interesting features can be observed from the curves shown in Fig. 10. In this experiment, the potential of a PbCaSn anode was swept from the rest potential to a positive limit of 2.05 V and then reversed to a negative-going limit of 1.2 V, reversed again to a positive limit of 2.05 V and so on as shown sequentially in the legend.

The first positive and negative sweeps are similar to those shown in Fig. 4. The second negative sweep (red curve) was limited to a potential of 1.6 V i.e. before reduction of PbO_2 to $PbSO_4$. The subsequent positive sweep (blue curve) showed that oxidation of iron(II) continued at its limiting current which decreased when the rotation of the electrode was interrupted at a potential of about 1.9 V before increasing again due to oxygen evolution. The final negative sweep shows a small limiting current (stationary electrode) but a more well-defined cathodic peak at 1.54 V due presumably to a greater residual amount of PbO_2 on the surface as a result of increased oxidation because of the higher positive potential limit and the reduced rate of reaction (5).

Open cicuit potential-time transients after oxidation of the PbCaSn alloy at various potentials (shown in Fig. 7) for 1 hour are shown in Fig. 11. After oxidation at 1.7 V for one hour in the absence of iron(II) in solution, the potential decays rapidly to about 1.55 V where it remains for about 30 seconds before decaying rapidly to a potential of about -0.2 V. The potential arrest at 1.55 V is probably due to reaction (3) in which the oxide layer oxidises the underlying lead metal to lead sulphate. This $PbSO_4$ layer at the interface prevents contact of the outer PbO_2 surface with the metal and the potential decays to the $Pb/PbSO_4$ potential.

In the presence of iron(II), the transients do not reveal an arrest for the reduction of PbO_2 at 1.55 V showing that the rate of reduction of PbO_2 by iron(II) is rapid. In addition a potential arrest is observed between 1.2 and 1.1 V the period of which decreases with increasing potential of oxidation. At anodization potentials of 1.85 V and above, this potential arrest is not clearly visible. In all cases, the

potential decays to values between 0.2 and 0.4 V where it remains for over an hour before a second transition to the $Pb/PbSO_4$ potential at -0.2 V.

These potential arrests were also observed after oxidation at potentials below about 1.85 V in a study of the anodic behaviour of a Pb-Ca alloy (Ruetschi and Angstadt, 1964) and interpreted by Ruetschi (1973) as being due to the PbO_2/PbO (1.13 V) and PbO/Pb (0.32 V) potentials within the membrane where the pH was estimated to be about 9.3. The fact that the potential arrest at 1.13 V decreases with increasing oxidation potential and is not observed in the presence of iron(II) after oxidation at potentials above 1.725 V could be due to the fact that iron(II) reduces the PbO_2 layer from the solution side of the membrane which is thicker (in terms of $PbSO_4$) at the low potentials and is completely oxidised to PbO_2 at the higher potentials.

3.3 Anodic reactions in the presence of iron(II) and manganese(II)

The effect of the addition of small amounts of manganese ions to the solution on the cyclic voltammograms of the PbCaSn anode in a solution containing 150 g L^{-1} H_2SO_4 and 5 g L^{-1} Fe(II) is shown in Fig. 12. The scans were started from the open circuit potential at about -0.35 V to positive potentials of about 2.05 V, and reversed.

The increased current in the potential region of 1.9 to 2.0 V in the presence of 1 g L^{-1} manganese is due to oxidation of manganese to higher oxidation states with the eventual formation of hydrated oxides of manganese (III) and (IV). In the presence of iron(II), reduction of these oxides together with that of PbO_2 is probable on the anode surface by the reaction

$$MnO_2 + 2Fe^{2+} + 4H^+ = Mn^{2+} + 2Fe^{3+} + 2H_2O \quad (6)$$

It appears from the curves in Fig. 12 that the apparent limiting current density for the oxidation of iron(II) decreases somewhat with increasing concentration of manganese. This is probably due to the fact that reaction (6) is occurring to some extent thereby reducing the limiting current for the competing electrochemical oxidation of iron(II). The shift of the potential at the edge of the plateau to lower potentials in the presence of manganese ions suggests that the presence of manganese oxides inhibits the reduction of PbO_2.

4. Practical Implications

The results of this study have shown that the rate of oxidation of iron(II) at the anodes in the electrowinning of copper is controlled by mass transport to the anode surface. Knowledge of the local mass transport coefficient thus enables a calculation to be made of the limiting current density for the oxidation of iron(II) and this will be the subject of a future study. During periods of power interruption to the tankhouse, iron(II) in the electrolyte will reduce the PbO_2 surface layer at the solution/layer interface to $PbSO_4$ while PbO_2 within the membrane will be similarly reduced to PbO by the alloy. Thus, iron(II) will enhance the rate of degradation of the protective oxide layer on the anode surface which will contribute to greater spalling of the layer and consequent higher lead contamination of the cathodes when power is resumed. The rates of these reactions have been shown to be relatively rapid and this degradation will occur even during short periods of power interruption during which time it would be advisable to switch off the circulation of the electrolyte through the cells.

5. Conclusions

This study of the oxidation of iron(II) on the surface of anodes used for the electrowinning of copper and zinc has shown some interesting and practically important results.

1. Oxidation of iron(II) does not occur on a $PbSO_4$ surface but occurs readily on a PbO_2 (and a "MnO_2") surface.

2. Oxidation of iron(II) occurs at the mass-transport controlled rate at the operating potentials of anodes during the electrowinning of copper.

3. Chemical reaction between iron(II) and PbO_2 on the surface of the anodes is rapid as is the rate of the reaction with MnO_2.

4. The presence of iron(II) in the electrolyte will increase the rate of "sulfation" of anodes during power disruptions in copper tankhouses.

6. References

Cifuentes, L., Glasner, R., 2003. Kinetics of the electrolytic ferrous to ferric ion oxidation on various anode materials. Revista de Metallurgia. 39, 260-267.

Dew, D.W., Phillips, C.V., 1985. The effect of Fe(II) and Fe(III) on the efficiency of copper electrowinning from dilute acid Cu(II) sulphate solutions with the chemelec cell: Part I. Cathodic and anodic polarisation studies. Hydrometallurgy. 14, 331-349.

El-Sherbiny, M.F., Zatout, A.A., Hussein, M., Sedahmed, G.H., 1991. Mass transfer at the gas evolving inner electrode of a concentric cylindrical reactor. J. Appl. Electrochem. 21, 537-542.

Kolodziej, B., Adamski, Z., 1985. Effect of manganese (II) added to the electrolyte on the properties of lead anodes used in oxidation of ferrous sulphate to ferric sulphate. J. Appl. Electrochem. 15, 705-710.

Li J., Miller, J.D., 2007. Reaction kinetics of gold dissolution in acid thiourea solution using ferric sulfate as oxidant. Hydrometallurgy. 89, 279-288.

Pavlov, D., Dinev, Z., 1980. Mechanism of the electrochemical oxidation of lead to lead dioxide electrode in sulfuric acid solution. J. Electrochem. Soc. 127, 855-863.

Ruetschi, P., 1973. Ion selectivity and diffusion potentials in corrosion layers. Lead sulfate films on lead in sulfuric acid. J. Electrochem. Soc. 120, 331-336.

Ruetschi, P., Angstadt, R.T., 1964. Anodic oxidation of lead at constant potential. J. Electrochem. Soc. 111, 1323-1330.

Sharpe, T.F., 1977. The behaviour of lead alloys as lead dioxide electrodes. J. Electrochem. Soc. 124, 168-173.

Tjandrawan, V., Nicol, M.J., 2010. The role of manganese in the electrowinning of copper. *Copper 2010*, GDMB, Claustal-Zellerfeld, Germany, vol 5, 1771-1782.

List of Figures

Fig. 10 Successive voltammetric scans of a Pb-Ca-Sn anode in a solution of 150 g L^{-1} H_2SO_4 and 5 g L^{-1} iron(II) at 800 rpm. Rotation speed reduced to zero at 1.9 V in penultimate sweep

Fig. 11 Open-circuit potential-time transients on a PbCaSn anode after oxidation at various potentials for 1 h in a solution of 150 g L^{-1} H_2SO_4 and 5 g L^{-1} iron(II) at 800 rpm. The curve at 1.7 V in the absence of iron(II) is also shown

Fig. 12 Voltammetric scans of Pb-Ca-Sn anode in solution of 150 g L^{-1} H_2SO_4 and 5 g L^{-1} iron(II) with various manganese concentrations

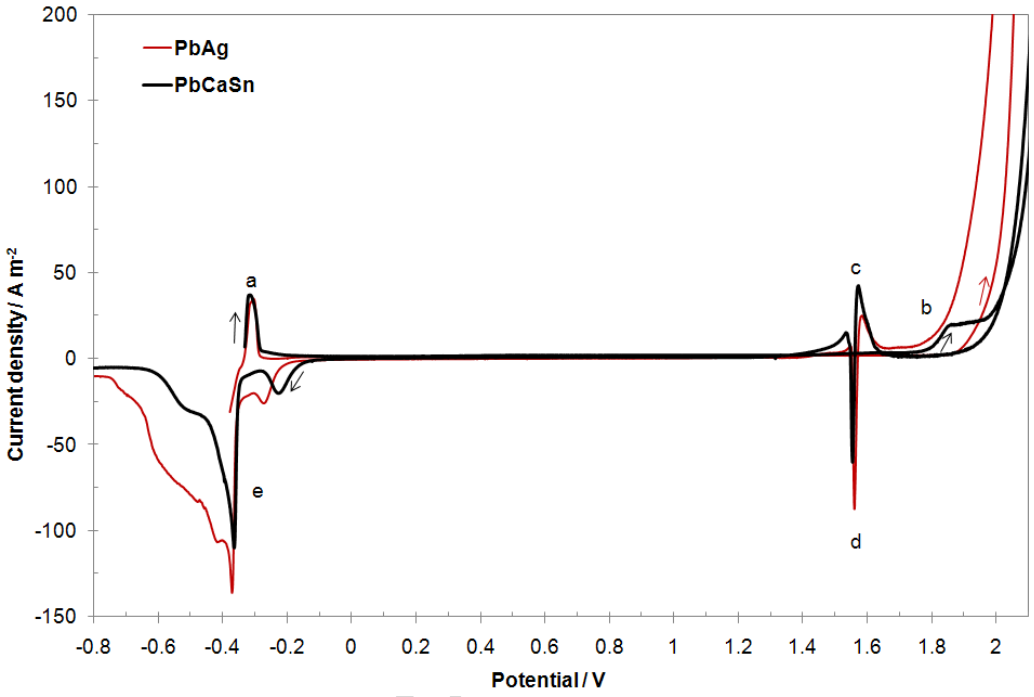

Fig. 1 Voltammetric scans of Pb-Ag and Pb-Ca-Sn anodes in a solution containing 150 g L^{-1} H_2SO_4

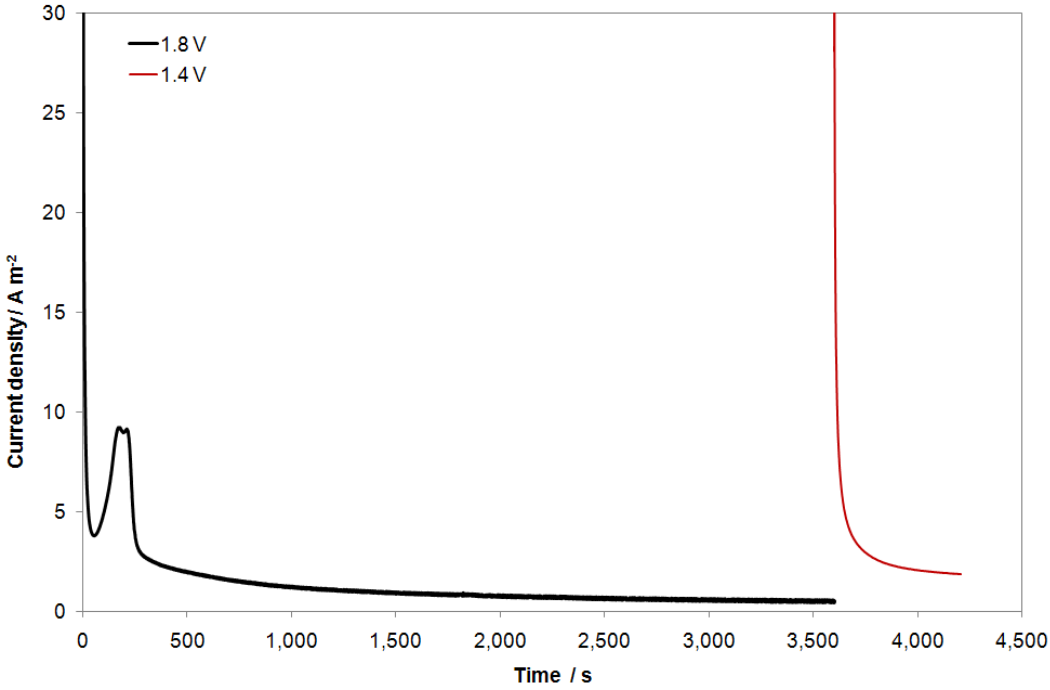

Fig. 2 Current-time transients for the oxidation of a PbCaSn anode held at 1.8 V in a solution containing 150 g L^{-1} H_2SO_4 for 1 hour after which the potential was reduced to 1.4 V

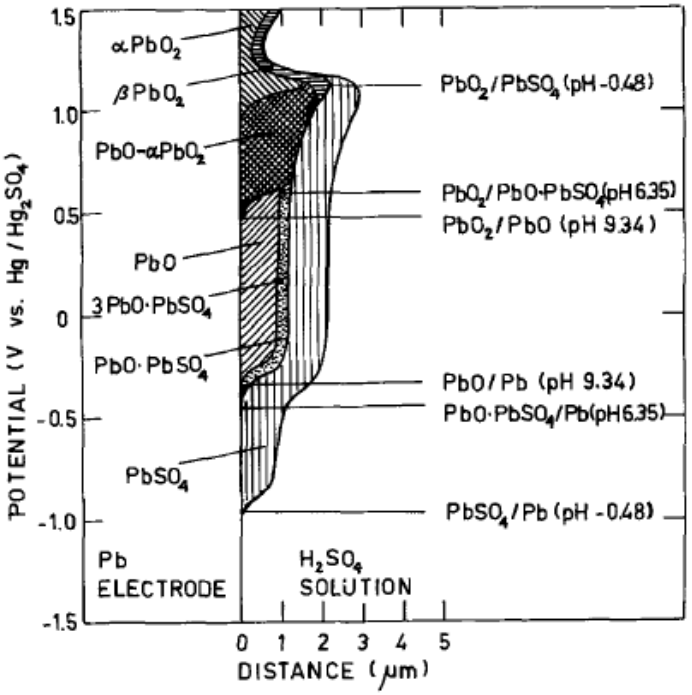

Fig. 3 Schematic representation of the multi-phase corrosion layer on a lead anode at different potentials. After Ruetschi (1973)

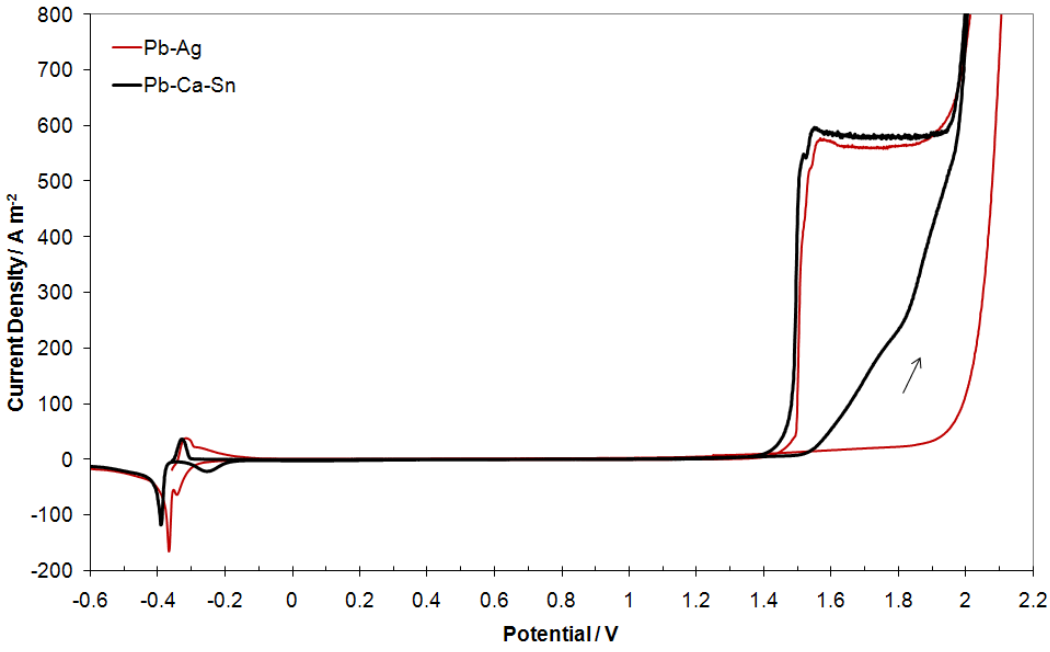

Fig. 4 Voltammetric scans of Pb-Ag and Pb-Ca-Sn anodes in a solution containing 150 g L^{-1} H_2SO_4 and 10 g L^{-1} iron(II)

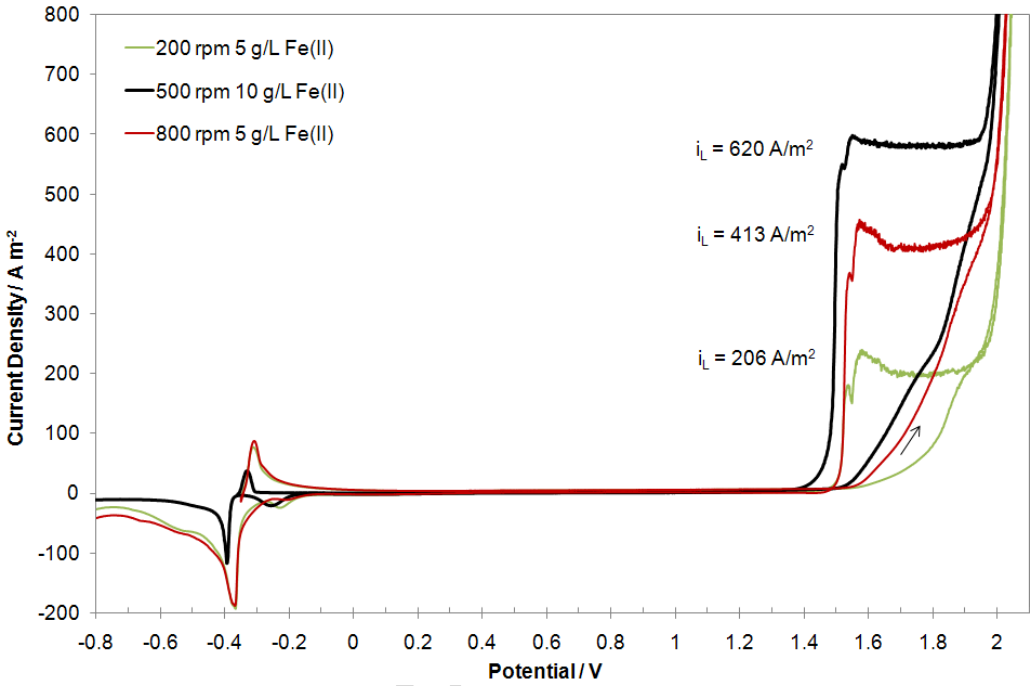

Fig. 5 Voltammetric scans of a Pb-Ca-Sn anode in solutions of 150 g L^{-1} H_2SO_4 and 5 or 10 g L^{-1} iron(II) at various rotation speeds. The limiting currents shown are calculated from the Levich equation

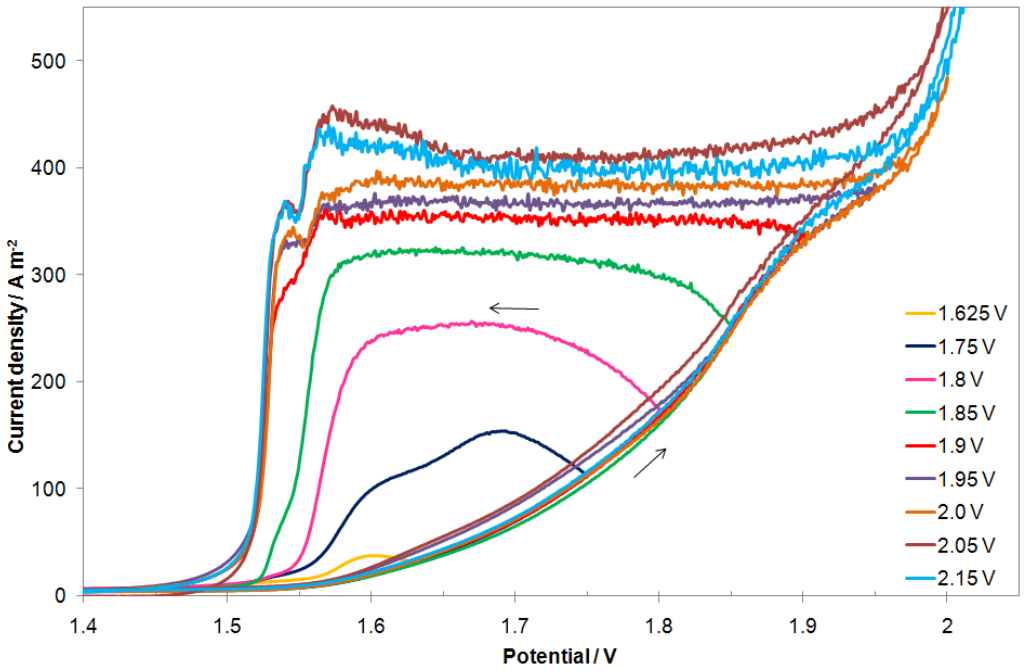

Fig. 6 Voltammetric scans of a Pb-Ca-Sn anode in a solution of 150 g L^{-1} H_2SO_4 and 5 g L^{-1} iron(II) at 800 rpm. The positive potential limit was increased in successive sweeps

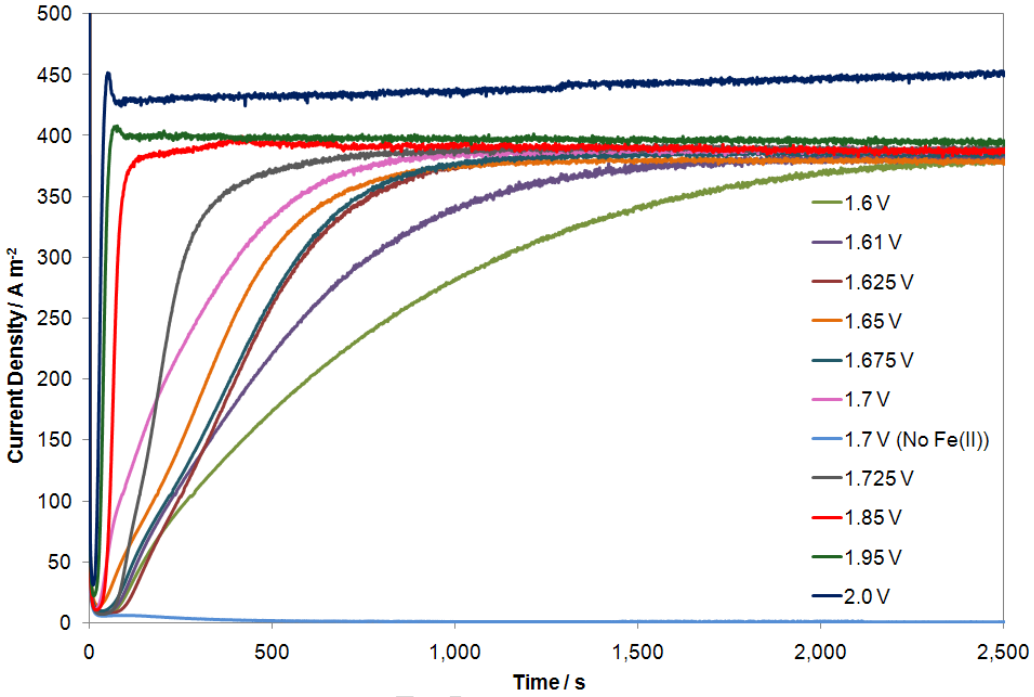

Fig. 7 Current-time transients for the oxidation of iron(II) on a PbCaSn alloy anode held at various potentials in a solution of 150 g L^{-1} H_2SO_4 and 5 g L^{-1} iron(II) at 800 rpm

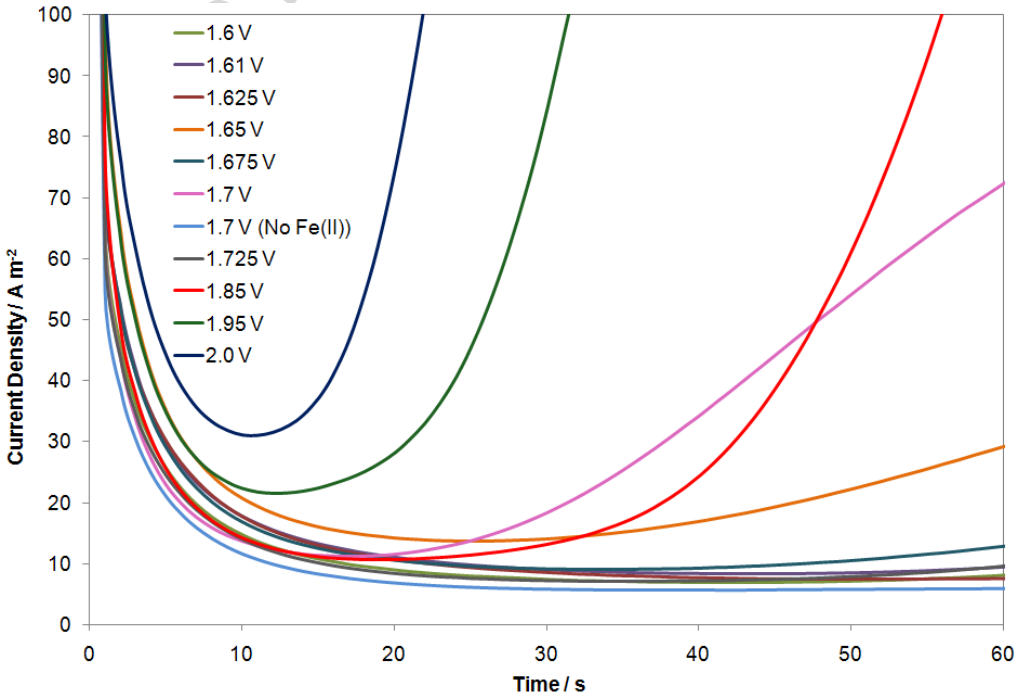

Fig. 8 Current-time transients for the initial stage of oxidation of iron(II) on a PbCaSn alloy anode held at various potentials in a solution of 150 g L^{-1} H_2SO_4 and 5 g L^{-1} iron(II) at 800 rpm

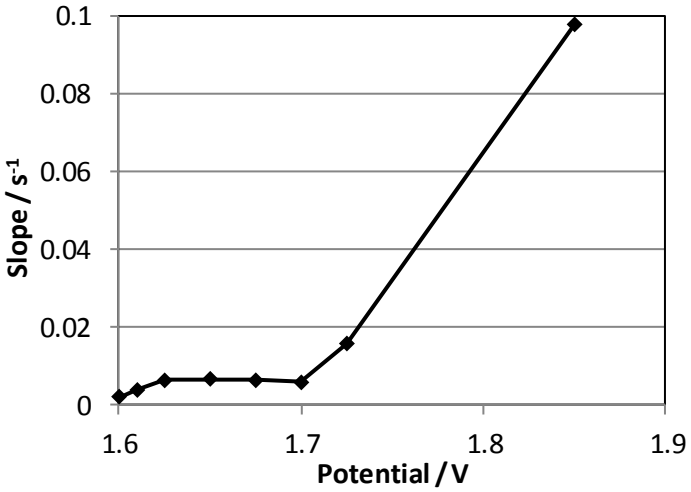

Fig. 9 Slopes of the plots of $\ln(1/i - 1/i_L)$ versus potential from the transients in Fig.7

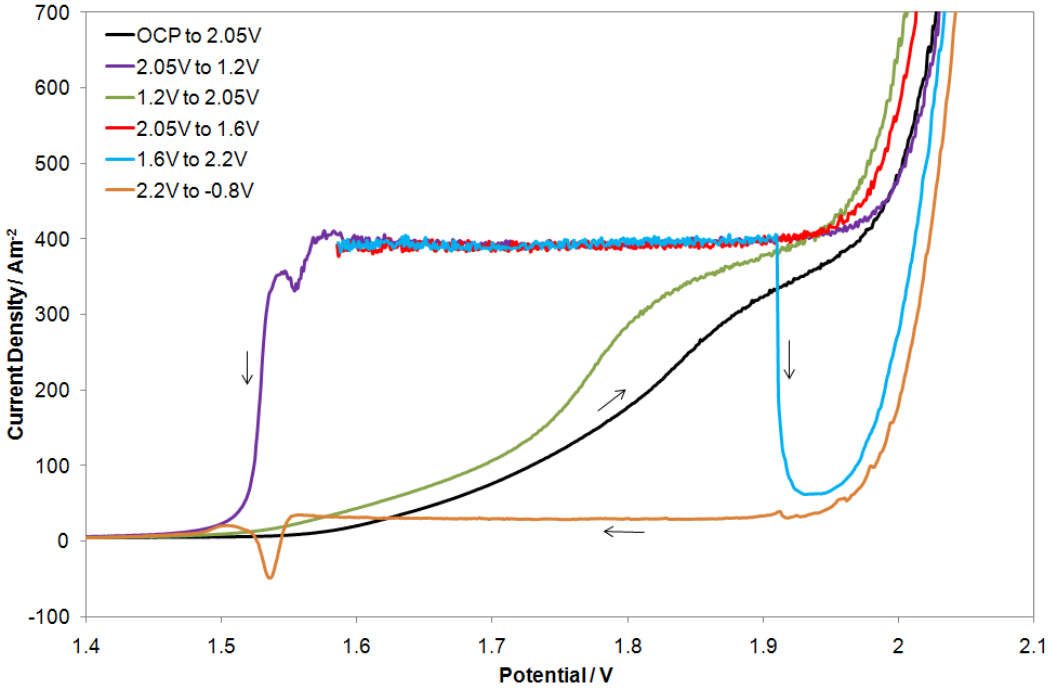

Fig. 10 Successive voltammetric scans of a Pb-Ca-Sn anode in a solution of 150 g L^{-1} H_2SO_4 and 5 g L^{-1} iron(II) at 800 rpm. Rotation speed reduced to zero at 1.9 V in penultimate sweep

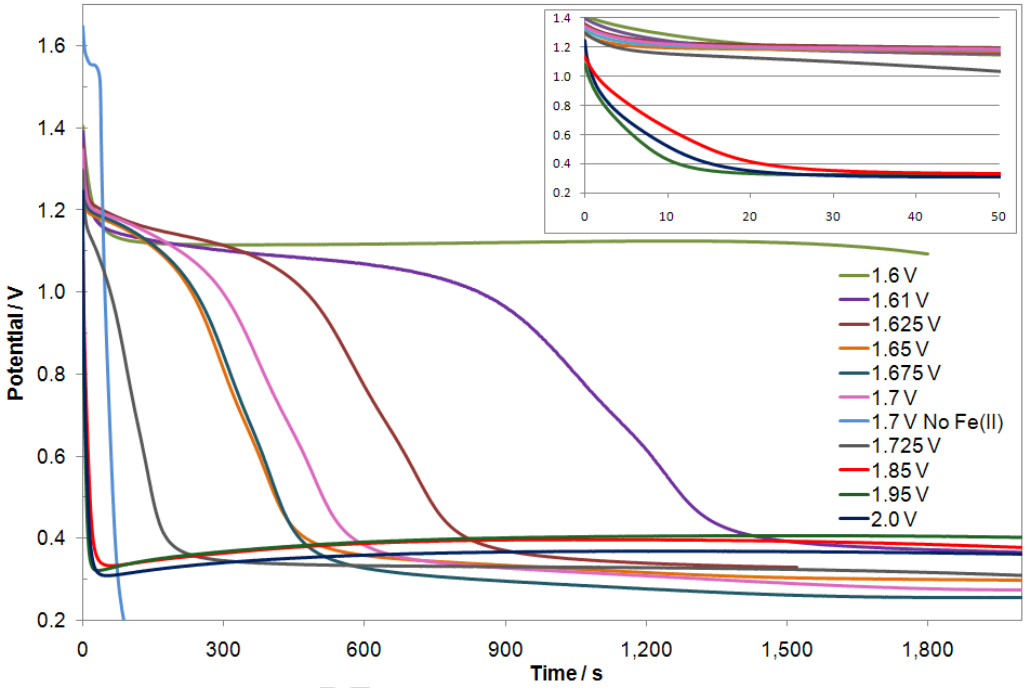

Fig. 11 Open-circuit potential-time transients on a PbCaSn anode after oxidation at various potentials for 1 h in a solution of 150 g L^{-1} H_2SO_4 and 5 g L^{-1} iron(II) at 800 rpm. The curve at 1.7 V in the absence of iron(II) is also shown

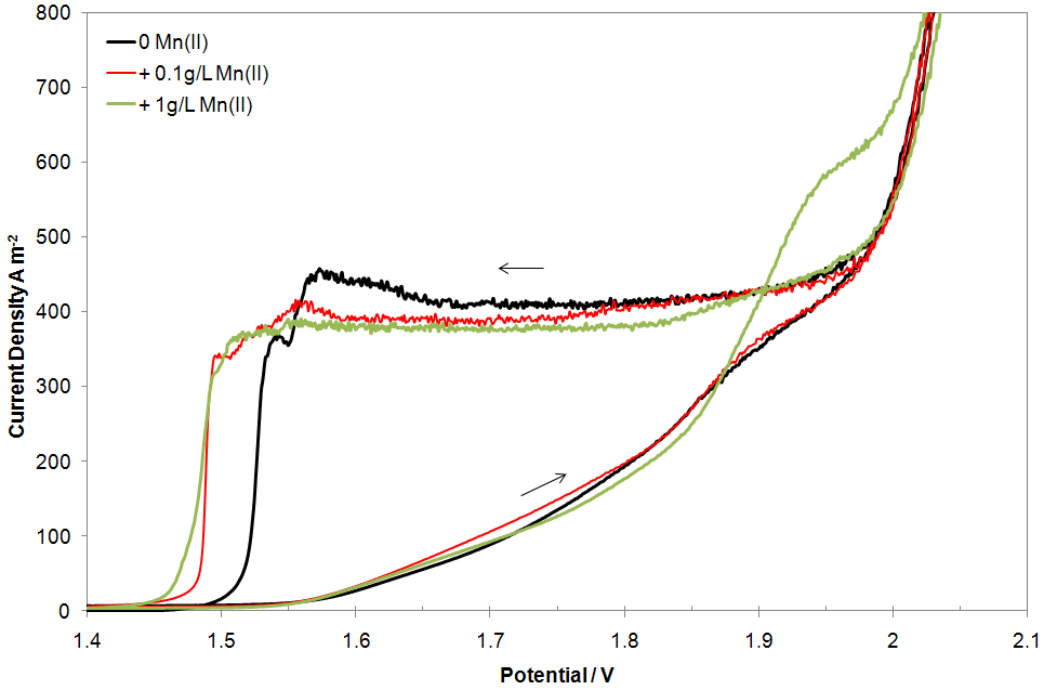

Fig. 12 Voltammetric scans of Pb-Ca-Sn anode in solution of 150 g L^{-1} H_2SO_4 and 5 g L^{-1} iron(II) with various manganese concentrations

Highlights

- Oxidation of iron(II) on Pb-Ca-Sn and Pb-Ag anodes does not occur on a lead sulphate surface but readily on lead dioxide.
- The rate of the oxidation of iron(II) is controlled by mass transport to the anode surface.
- Chemical reaction between iron(II) and PbO_2 on the surface is rapid.
- Oxidation of iron(II) also occurs on the surface of manganese oxides which can also rapidly oxidise iron(II).
- The presence of iron(II) increases the rate of "sulfation" of anodes during power disruptions.